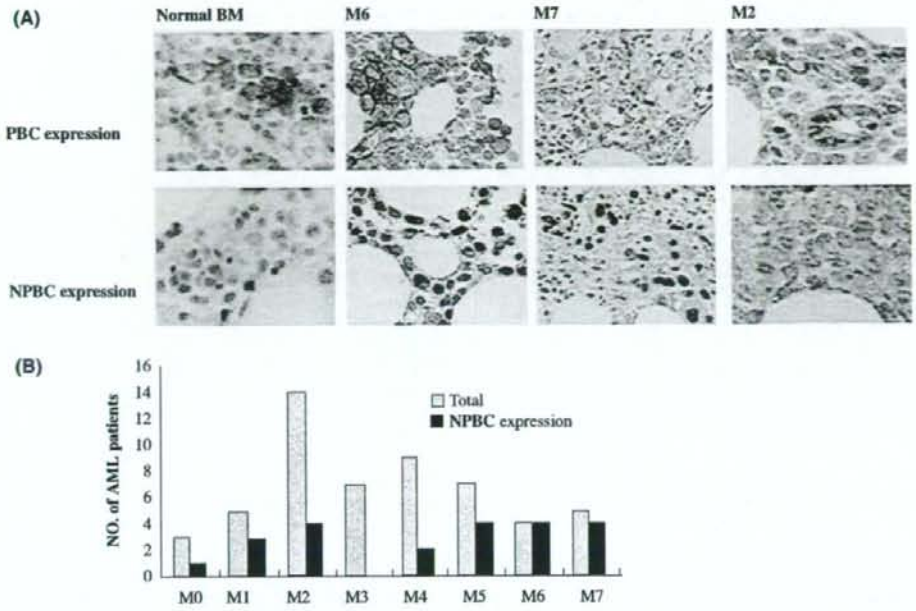

Fig 1. Specific association of NPBC expression with FAB subtypes of AML specimens. (A) In normal BM clots, PBC is expressed on the membranes of erythroid cells as well as endothelial cells. NPBC was not detected in normal BM clots. Most erythroid cells and endothelial cells showed cell membrane expression of PBC without expression in the nucleus or cytoplasm. NPBC was expressed in leukemia cells and was always restricted to the nucleus, especially in M6 and M7 specimens. Prominent staining of endothelial cells was seen in the vascular tissue in BM derived from an M2 patient with, though NPBC staining was negative in the same specimen. Original magnification ×40. (B) The graph presents data based on nuclear NPBC staining in paraffin sections from 54 patients with AML.

samples except for M3 (Fig 3A). The anti-N-terminal nonphosphorylated peptide antibody gave bands of the same size in only a few samples of AML and MDS (Fig 3B). The results of immunoblotting corresponded to those of immunostaining, although the latter was more sensitive than the former.

The above findings suggest that expression of nuclear NPBC could be used to identify some subsets of AML and MDS. Next we studied whether nuclear NPBC was associated with chromosomal abnormalities or genetic alterations. Previous studies suggested that AML-associated translocations, such as t(8;21) and t(15;17), contributed to the activation of gamma-catenin, or that *FLT3* mutation might be associated with the stabilization of beta-catenin. In this study, however, nuclear NPBC was never detected in AML with t(8;21) or t(15;17). In AML/MDS with −7/−7q and a complex karyotype, nuclear NPBC was frequently detected ($P = 0{\cdot}007$ and $P = 0{\cdot}02$, respectively; Table II). Moreover, detection was not related to *FLT3* internal tandem duplication (ITD; Table II).

Finally, we studied whether clinical characteristics and outcome were different between nuclear NPBC$^+$ and NPBC$^-$ AML patients. NPBC$^+$ AML patients showed significantly lower hemoglobin levels, lower blast percentages in the BM, and lower CR rates (Table I). There were no significant differences between the NPBC$^+$ and NPBC$^-$ groups in the MDS patients (Table I). However, nuclear NPBC was associated with a high International Prognostic Scoring System (IPSS) score (Table I). Of note, nuclear NPBC$^+$ AML patients had worse overall survival than NPBC$^-$ AML patients (Fig 4A). Even if the M6/M7 subtype and/or M3 subtype was excluded from the analysis, there was still a significant association between nuclear NPBC$^+$ and survival (Fig 4B–D).

Discussion

This study used nuclear NPBC as a biomarker for the activated Wnt/beta-catenin signaling pathway. The anti-beta-catenin C-terminal peptide antibody detected total beta-catenin in immunoblots but mainly cytoplasmic and membrane-associated beta-catenin in immunohistological analysis, whereas the anti-beta-catenin N-terminal nonphospholylated peptide antibody detected only nuclear beta-catenin in both analyses (data not shown). Accordingly, it was concluded that the nuclear staining with the latter antibody identified nuclear non-phosphorylated beta-catenin. Nuclear NPBC was detected in 22 (40·7%) of 54 AML patients and 18 (40·9%) of 44 MDS patients. Positive staining of nuclear NPBC was associated with particular AML subtypes (M6 and M7), a low complete remission rate, and poor prognosis. The presence of nuclear

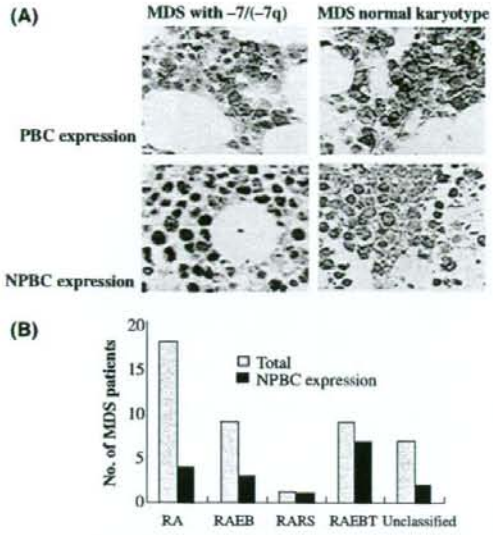

Fig 2. Specific association of NPBC expression with FAB subtypes of MDS specimens. (A) Most erythroid cells and endothelial cells showed cell membrane expression of PBC without expression in the nucleus or cytoplasm. NPBC was expressed in erythroid cells and was always restricted to the nucleus, especially in refractory anaemia with excess blasts in transformation (RAEBT) and MDS specimens with −7/−7(q). Original magnification ×40. (B) The graph presents data obtained for nuclear NPBC staining in paraffin sections from 44 patients with MDS. RA, refractory anaemia; RARS, RA with ringed sideroblasts; RAEB, RA with excess blasts.

NPBC was also associated with a high IPSS score of MDS and with −7/−7q and complex karyotypes.

Previous reports indicated that a significant proportion of AML samples expressed beta-catenin on immunoblot analysis.

Table II. Cytogenetic abnormalities and *FLT3* mutation according to nuclear NPBC expression.

	Nuclear NPBC$^+$ (*N*)	Nuclear NPBC$^-$ (*N*)	*P*-value
Karyotypes			
t(8;21)	0	3	NS
t(15;17)	0	4	NS
−5/−5q	4	1	NS
−7/−7q	12	6	0·007
Complex	13	7	0·02
Others	19	2	NS
Normal	10	31	0·0003
Unknown	7	1	0·02
FLT3 mutation			
Wild type	3	12	0·006
ITD	2	5	NS

Patients are counted more than once due to the coexistence of more than one cytogenetic abnormality. Complex: patients had three or more cytogenetic abnormalities.
NPBC, non-phosphorylated beta-catenin; ITD, internal tandem repeat; NS, not significant.

The expression of beta-catenin is related to CD34 expression, poor prognosis and clonogenic capacity *ex vivo* (Ysebaert *et al*, 2006). Furthermore, beta-catenin is expressed in normal CD34$^+$ progenitor cells and the expression level is reduced upon differentiation (Simon *et al*, 2005). In these studies, however, the total beta-catenin level was analyzed only by immunoblot analysis. Beta-catenin is expressed not only as nuclear NPBC but also as a cadherin-associated protein in the inner cytomembrane (Conacci-Sorrell *et al*, 2002). The present study found that normal erythroblasts expressed cytoplasmic or membrane-associated beta-catenin but not nuclear NPBC (Fig 1A). Both membrane-associated and nuclear beta-catenin was expressed in malignant erythroblasts in subtype M6

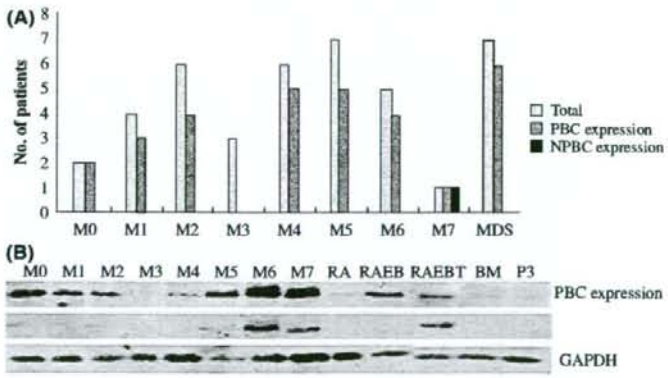

Fig 3. Beta-catenin expression of AML cells assessed by immunoblotting. (A) The graph shows data obtained for the expression of NPBC in mononuclear cells from 41 patients with AML, and the data indicate that expression of NPBC is specific to some FAB subtypes, especially to M6 and M7. (B) Representative immunoblots for PBC and NPBC in AML samples. RA, refractory anaemia; RARS, RA with ringed sideroblasts; RAEB, RA with excess blasts; RAEBT, refractory anaemia with excess blasts in transformation.

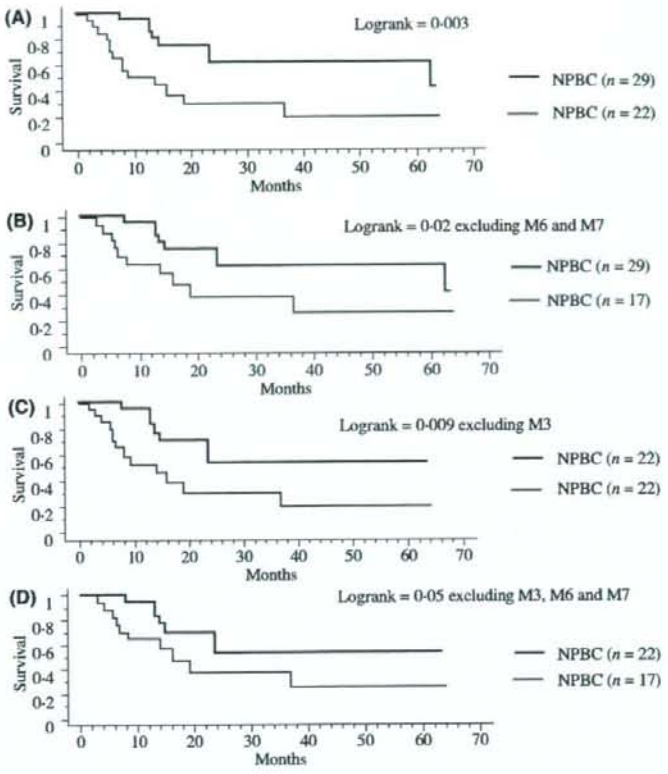

Fig 4. Kaplan–Meier cumulative survival curves were calculated for 51 AML patients (A) and 46 patients excluding subtype M6/M7 (B), 44 patients excluding subtype M3 (C), 39 patients excluding subtype M3/M6/M7 (D), respectively, according to the presence of nuclear NPBC. Comparison of the survival curves using the log-rank test identified nuclear NPBC$^+$ as a prognostic factor.

(Fig 1A). These findings suggest that increased nuclear NPBC levels were the result of aberrant signal transduction in the Wnt pathway or an abnormality of beta-catenin itself.

In this study, the expression levels of total and non-phosphorylated beta-catenin were correlated but varied significantly among leukemia samples. In M6 and M7 samples, the expression of beta-catenin was significantly augmented, whereas it was hardly detected in M3 and normal BM samples. These variations suggest the possibility that Wnt/beta-catenin signaling is mediated by multiple factors, such as immaturity, lineage, and oncogenic signals.

We established a correlation between nuclear NPBC$^+$ and poor survival in AML patients. The prognostic value of total beta-catenin expression has been previously studied in AML patients (Ysebaert *et al*, 2006), but the present study clearly showed for the first time that nuclear NPBC is associated with prognosis. The association was still observed even if M6/M7 and/or M3 patients were excluded from the analysis. Nuclear NPBC might be a new prognostic marker for AML and MDS that can be evaluated by histopathological examination.

Wnts are a family of paracrine and autocrine factors that regulate cell growth and cell fate (Reya *et al*, 2003). The Wnt autocrine signaling mechanism was initially discovered in human breast and ovarian tumor cell lines as well as in MM primary samples (Bafico *et al*, 2004; Derksen *et al*, 2004). Since several Wnt family members have been reported in BM stromal cells, it is possible that leukaemia cells respond to different proteins of the Wnt/beta-catenin pathway secreted by stromal cells in a paracrine fashion (Austin *et al*, 1997; Van Den Berg *et al*, 1998; Etheridge *et al*, 2004). Nuclear NPBC was detected in some cell lines only when they were transplanted in non-obese diabetic/severe combined immunodeficient/gammacnull (NOG) mice (data not shown). Thus, the leukaemia niche may have an important role in nuclear NPBC expression during AML.

MDS is a clonal hematopoietic stem cell disorder characterized by multi-lineage dysplasia and pancytopenia in which further genetic events may be required for the rapid expansion of leukaemic blasts (Heaney & Golde, 1999; Hirai, 2003). Although nuclear NPBC has been studied in many cancers as

well as haematological malignancies, it has not been studied in MDS (Morin *et al*, 1997; Barker & Clevers, 2000; Giles *et al*, 2003). This is the first study to report the expression of beta-catenin in MDS patients. Here we showed that nuclear NPBC was related to the IPSS score and that secondary AML from MDS showed the highest percentage of nuclear NPBC expression. The Wnt signaling pathway may play an important role in the pathogenesis of the transformation of MDS into AML. Regarding chromosomal abnormalities, −7/−7q and/or complex karyotypes were significantly associated with the presence of nuclear NPBC. According to recent data (Liu *et al*, 2006), the gene encoding alpha-catenin (*CTNNA1*) is suppressed by deletion and/or methylation. Both alpha-catenin and beta-catenin bind to the inner membrane of hematopoietic cells, and cadherin binds to actin filaments via the catenin complex. If the expression of alpha-catenin is suppressed in the 5q- genotype or for other reasons, beta-catenin may be abnormally located or activated. In this study, abnormalities of chromosome 5 were associated with the presence of NPBC but this was not statistically significant. The reason why NPBC is associated with chromosome 7 abnormalities remains unclear. A gene encoded by chromosome 7 may be associated with the regulation of the Wnt/beta-catenin pathway. Several possible candidate genes including *SFRP4*, *WNT2*, and *FZD1* and *FZD9* are located at human chromosome 7. There are reports that sFRP4 plays a role in tumor suppression via the Wnt pathway (Hrzenjak *et al*, 2004; Horvath *et al*, 2007), although the specific relationship remains unknown. Since many molecules are directly or indirectly associated with the phosphorylation, stabilization and nuclear translocation of beta-catenin, the presence of nuclear NPBC might provide a clue to find a new leukemia-associated signaling mechanism.

In conclusion, *in situ* detection of nuclear NPBC by immunohistochemistry of paraffin sections from BM specimens could be used to predict the prognosis of AML and MDS. Understanding the mechanisms leading to leukemogenesis in nuclear NPBC$^+$ AML and MDS may lead to new anti-leukemia therapies.

Acknowledgements

This study is partly supported by Grants-in-Aid from National Institute of Biomedical Innovation and from Ministry of Education, Culture, Sports, Science and Technology on the Scientific Research. We thank Kazuko Matsuba for technical assistance, and Mari Otsuka for secretarial assistance.

References

Austin, T.W., Solar, G.P., Ziegler, F.C., Liem, L. & Matthews, W. (1997) A role for the Wnt gene family in hematopoiesis: expansion of multilineage progenitor cells. *Blood*, **89**, 3624–3635.

Bafico, A., Liu, G., Goldin, L., Harris, V. & Aaronson, S.A. (2004) An autocrine mechanism for constitutive Wnt pathway activation in human cancer cells. *Cancer Cell*, **6**, 497–506.

Barker, N. & Clevers, H. (2000) Catenins, wnt signaling and cancer. *BioEssays*, **22**, 961–965.

Bienz, M. & Clevers, H. (2000) Linking colorectal cancer to Wnt signaling. *Cell*, **103**, 311–320.

Chung, E.J., Hwang, S.G., Nguyen, P.M., Lee, S., Kim, J.S., Kim, J.W., Henkart, P.A., Bottaro, D.P., Soon, L.L., Bonvini, P., Lee, S.J., Karp, J.E., Oh, H.J., Rubin, J.S. & Trepel, J.B. (2002) Regulation of leukemic cell adhesion, proliferation and survival by beta-catenin. *Blood*, **100**, 982–990.

Cobas, M., Wilson, A., Ernst, B., Mancini, S.J.C., MacDonald, H.R., Kemler, R. & Radtke, F. (2004) Catenin is dispensable for hematopoiesis and lymphopoiesis. *Journal of Experimental Medicine*, **199**, 221–229.

Conacci-Sorrell, M., Zhurinsky, J. & Ben-ZeÀfev, A. (2002) The cadherin-catenin adhesion system in signaling and cancer. *Journal of Clinical Investigation*, **109**, 987–991.

Derksen, P.W.B., Tjin, E., Meijer, H.P., Klok, M.D., Mac Gillavry, H.D., Oers, M.H.J.V., Lokhorst, H.M., Bloem, A.C., Clevers, H., Nusse, R., Neut, R.V.D., Spaargaren, M. & Pals, S.T. (2004) Illegitimate WNT signaling promotes proliferation of multiple myeloma cells. *Proceedings of the National Academy of Sciences of the United States of America*, **101**, 6122–6127.

Etheridge, S.L., Spencer, G.J., Heath, D.J. & Genever, P.G. (2004) Expression profiling and functional analysis of wnt signaling mechanisms in mesenchymal stem cells. *Stem Cells*, **22**, 849–860.

Giles, R.H., van Es, J.H. & Clevers, H. (2003) Caught up in a Wnt storm: Wnt signaling in cancer. *Biochimica et Biophysica Acta*, **1653**, 1–24.

He, T.C., Sparks, A.B., Rago, C., Hermeking, H., Zawel, L., da Costa, L.T., Morin, P.J., Vogelstein, B. & Kinzler, K.W. (1998) Identification of c-MYC as a target of the APC pathway. *Science*, **281**, 1509–1512.

Heaney, M.L. & Golde, D.W. (1999) Articles medical progress: myelodysplasia. *New England Journal of Medicine*, **340**, 1649–1660.

Hirai, H. (2003) Molecular mechanisms of myelodysplastic syndrome. *Japanese Journal of Clinical Oncology*, **33**, 153–160.

Horvath, L.G., Lelliott, J.E., Kench, J.G., Lee, C.S., Williams, E.D., Saunders, D.N., Grygiel, J.J., Sutherland, R.L. & Henshall, S.M. (2007) Secreted frizzled-related protein 4 inhibits proliferation and metastatic potential in prostate cancer. *Prostate*, **67**, 1081–1090.

Hrzenjak, A., Tippl, M., Kremser, M.L., Strohmeier, B., Guelly, C., Neumeister, D., Lax, S., Moinfar, F., Tabrizi, A.D., Isadi-Moud, N., Zatloukal, K. & Denk, H. (2004) Inverse correlation of secreted frizzled-related protein 4 and -catenin expression in endometrial stromal sarcomas. *The Journal of Pathology*, **204**, 19–27.

Jamieson, C.H.M., Ailles, L.E., Dylla, S.J., Muijtjens, M., Jones, C., Zehnder, J.L., Gotlib, J., Li, K., Manz, M.G., Keating, A., Sawyers, C.L. & Weissman, I.L. (2004) Granulocyte-macrophage progenitors as candidate leukemic stem cells in blast-crisis CML. *New England Journal of Medicine*, **351**, 657–667.

Liu, T.X., Becker, M.W., Jelinek, J., Wu, W.S., Deng, M., Mikhalkevich, N., Hsu, K., Bloomfield, C.D., Stone, R.M., DeAngelo, D.J., Galinsky, I.A., Issa, J.P., Clarke, M.F. & Look, A.T. (2006) Chromosome 5q deletion and epigenetic suppression of the gene encoding -catenin (CTNNA1) in myeloid cell transformation. *Nature Medicine*, **13**, 78–83.

Morin, P.J., Sparks, A.B., Korinek, V., Barker, N., Clevers, H., Vogelstein, B. & Kinzler, W.K. (1997) Activation of beta-catenin-Tcf signaling in colon cancer by mutations in beta-catenin or APC. *Science*, **275**, 1787–1790.

Noort, M.V., Meeldijk, J., Zee, R.V.D., Destree, O. & Clevers, H. (2002) Wnt signaling controls the phosphorylation status of beta-catenin. *Journal of Biological Chemistry*, **277**, 17901–17905.

Ozeki, K., Kiyoi, H., Hirose, Y., Iwai, M., Ninomiya, M., Kodera, Y., Miyawaki, S., Kuriyama, K., Shimazaki, C., Akiyama, H., Nishimura, M., Motoji, T., Shinagawa, K., Takeshita, A., Ueda, R., Ohno, R., Emi, N. & Naoe, T. (2004) Biologic and clinical significance of the FLT3 transcript level in acute myeloid leukemia. *Blood*, **103**, 1901–1908.

Polakis, P. (2000) Wnt signaling and cancer. *Genes and Development*, **14**, 1837–1851.

Reya, T., Duncan, A.W., Ailles, L., Dome, J., Scherer, D.C., Willert, K., Hintz, L., Nusse, R. & Weissman, I.L. (2003) A role for Wnt signaling in self-renewal of hematopoietic stem cells. *Nature*, **423**, 409–414.

Serinsöz, E., Neusch, M., Büsche, G., Wasielewski, R.V., Kreipe, H. & Bock, O. (2004) Aberrant expression of beta-catenin discriminates acute myeloid leukaemia from acute lymphoblastic leukaemia. *British Journal of Haematology*, **126**, 313–319.

Simon, M., Grandage, V.L., Linch, D.C. & Khwaja, A. (2005) Constitutive activation of the Wnt/beta-catenin signalling pathway in acute myeloid leukaemia. *Oncogene*, **24**, 2410–2420.

Staal, F.J.T., Noort, M.V., Strous, G.J. & Clevers, H.C. (2002) Wnt signals are transmitted through N-terminally dephosphorylated beta-catenin. *EMBO Reports*, **3**, 63–68.

Tetsu, O. & Maccormick, F. (1999) Catenin regulates expression of cyclin D1 in colon carcinoma cells. *Nature*, **398**, 422–426.

Tickenbrock, L., Schwable, J., Wiedehage, M., Steffen, B., Sargin, B., Choudhary, C., Brandts, C., Berdel, W.E., Tidow, C.M. & Serve, H. (2005) Flt3 tandem duplication mutations cooperate with Wnt signaling in leukemic signal transduction. *Blood*, **105**, 3699–3706.

Van Den Berg, D.J., Sharma, A.K., Bruno, E. & Hoffman, R. (1998) Role of members of the Wnt gene family in human hematopoiesis. *Blood*, **92**, 3189–3202.

Willert, K., Brown, J.D., Danenberg, E., Duncan, A.W., Weissman, I.L., Reya, T., Yates, J.R. & Nusse, R. (2003) Wnt proteins are lipid-modified and can actas stem cell growth factors. *Nature*, **423**, 448–452.

Xu, J.L., Lai, R., Kinoshita, T., Nakashima, N. & Nagasaka, T. (2002) Proliferation, apoptosis and intratumoral vascularity in multiple myeloma: correlation with the clinical stage and cytologic grade. *Journal of Clinical Pathology*, **55**, 530–534.

Ysebaert, L., Chicanne, G., Demur, C., Toni, F.D., Houdellier, N.P., Ruidavets, J.B., Mas, V.M.D., Huguet, F.R., Laurent, G., Payrastre, B., Manenti, S. & Sultan, C.R. (2006) Expression of beta-catenin by acute myeloid leukemia cells predicts enhanced clonogenic capacities and poor prognosis. *Leukemia*, **20**, 1211–1216.

Leukemia Research xxx (2008) xxx–xxx

Contents lists available at ScienceDirect

Leukemia Research

journal homepage: www.elsevier.com/locate/leukres

Brief communication

Evaluation of cardiac iron overload in transfusion-dependent adult marrow failure patients by magnetic resonance imaging

Jinho Park[a], Kazuma Ohyashiki[b,*], Soichi Akata[a], Kenichi Takara[a], Ritsuko Uno[a], Dai Kakizaki[a], Keisuke Miyazawa[b], Yukihiko Kimura[b], Koichi Tokuuye[a]

[a] Department of Radiology, Tokyo Medical University, Tokyo 160-0023, Japan
[b] First Department of Internal Medicine (Division of Hematology), Tokyo Medical University, 6-7-1 Nishishinjuku, Shinjuku-ku, Tokyo 160-0023, Japan

ARTICLE INFO

Article history:
Received 2 September 2008
Received in revised form 14 October 2008
Accepted 20 October 2008

Keywords:
Iron overload
Myocardial evaluation
MRI
Transfusion-dependent

ABSTRACT

We investigated magnetic resonance imaging T2-star (MRI-T2*) values and left ventricular ejection fraction (LVEF) in 7 adult patients with bone marrow failure with heavy transfusion to elucidate the correlation between cardiac iron overload and dysfunction. We demonstrated a positive correlation between the total volume of red blood cells (RBC) transfusion and ejection fraction. The normal T2* limit value, which represents cardiac siderosis, is probably 200 mL/kg RBC transfusion. Patients with serum ferritin levels of under 5000 ng/mL and who received 200–400 mL/kg RBC transfusion showed mild but progressive decrease of the T2* value without obvious reduction of the ejection fraction, indicating that the T2* value of MRI could be a predictor for cardiac iron deposition before the appearance of myocardial dysfunction. Transfused RBC amount of >400 mL/kg or rapid elevation of ferritin level of >5000 ng/mL might be warning sign for critical cardiac dysfunction. Since iron overload of the heart is a major factor affecting co-morbidity of bone marrow failure, MRI evaluation of cardiac iron overload and functional disturbance in adult non-thalassemic patients is essential.

1. Introduction

Iron overload is a major problem in managing patients with bone marrow failure syndromes, since it has been clarified that cardiac dysfunction is a major life-threatening co-morbidity [1]. Takatoku et al. demonstrated that most of the deaths of iron overload adult patients with marrow failure syndromes were due to infection and leukemia; while cardiac and liver failure were noted in 24.0% and 6.7%, respectively [1]. Therefore, early detection of cardiac iron overload before apparent cardiac dysfunction, and chelation therapy for patients receiving heavy transfusion with acquired anemia is recommended. In the past, a limited number of studies regarding myocardial iron overload in adult patients with transfusion-dependent acquired anemias have been published [2–7]. Some reports suggested that the cardiac magnetic resonance imaging T2-star (MRI-T2*) technique could be useful in determining cardiac iron overload [3,7], while the efficacy of MRI is still controversial [2]. We, therefore, planned to address this relevant clinical issue.

2. Materials and methods

2.1. Patients

We studied 7 adult patients with hematologic diseases, all of whom were transfusion-dependent. Total red cell transfusion value at the time of MRI evaluation ranged from 64 (12,800 mL) to 242 (48,400 mL) Japanese units (1 unit = 200 mL) of red blood cells (RBC). Serum ferritin levels ranged from 2868 ng/mL to 17,547 ng/mL at the time of the MRI study. Of the 7 patients, 2 each was given a diagnosis of diabetes mellitus or liver dysfunction (Table 1). None of the patients in this study received oral chelation therapy, but all of them received intermittent intravenous deferoxamine therapy.

2.2. MRI evaluation

We used a Magnetom Avanto 1.5 T scanner (Siemens AG, Erlangen, Germany) using a gradient echo T2* MRI technique. Gradient echo (GRE) T2*WI, and true-fast imaging with steady-state procession (true FISP) sequence was applied for a single mid-ventricular short-axis slice of the left cardiac ventricle at seven echo times (5 ms, 7 ms, 10 ms, 13 ms, 15 ms, 17 ms and 20 ms). The repeat time between each radiofrequency pulse was 170 ms. Phased array coils, electrocardiogram (ECG) gating, and breath holding methods were also utilized. We selected the short-axis of the left cardiac ventricle and applied true-FISP sequence to obtain cine MRI.

All MRI data were analyzed using Argus soft ware (Siemens AG) to calculate left ventricular ejection fraction (LVEF). Regions of interest (ROI) were set to the left ventricle wall. Measured signal intensity was fitted for an exponential curve and we obtained the T2* value of the myocardium. Axial T2*WI of upper abdomen was also obtained to determine the amounts of iron deposition in other organs, including the liver, pancreas, spleen, and vertebrae.

* Corresponding author. Tel.: +81 3 3342 1510; fax: +81 3 5381 6651.
E-mail address: ohyashik@rr.iij4u.or.jp (K. Ohyashiki).

0145-2126/$ – see front matter © 2008 Elsevier Ltd. All rights reserved.
doi:10.1016/j.leukres.2008.10.018

Please cite this article in press as: Park J, et al. Evaluation of cardiac iron overload in transfusion-dependent adult marrow failure patients by magnetic resonance imaging. Leuk Res (2008), doi:10.1016/j.leukres.2008.10.018

Table 1
Clinico-hematologic characteristics of patients with iron overload.

UPN	Age (yo)/sex	Diagnosis	Hb (g/dL)	Platelets ($\times 10^6$/L)	Total RBC transfusion (Japanese unit)	Serum ferritin (ng/mL)	Fe (μg/dL)	T2* value (ms)	LVEF (%)
1	56/male	MDS-RAEBt	7.7	31	12,800 mL (64)	3,056	171	94.34	61
2	71/female	MDS-RA	5.1	158	32,000 mL (160)	16,987	334	ND	52.8
3	66/male	MDS-RA	7.9	15	23,200 mL (116)	3,856	ND	35.71	63
4	37/female	AA	7.9	3	48,400 mL (242)	17,547	379	11.55	26.5
5	52/female	AA	8.2	11	>12,800 mL (>64)	3,441	233	50	54.8
6	77/male	PMF	7.2	34	11,600 mL (58)	2,868	152	51.02	59.5
7	71/male	PMF	4.6	212	24,000 mL (120)	3,176	300	35.59	61.3

Disease: MDS-RA, myelodysplastic syndrome-refractory anemia; MDS-RAEBt, myelodysplastic syndrome-refractory anemia with excess blasts in transformation; AA, aplastic anemia; PMF, primary myelofibrosis. Patient 5 had a diagnosis at childhood, thus exact transfused amount is unclear.

3. Results

Left ventricular ejection fraction in the 7 patients ranged from 26.5% to 63% (normal range: 56–78% by MRI), with 3 (patient nos. 2, 4, and 5) of them being below the normal range. Two (patient nos. 2 and 4) of the 3 patients with reduced LVEF levels had heavy RBC transfusion of >160 Japanese units and the serum ferritin levels were >15,000 ng/mL. Although the remaining 4 transfusion-dependent patients showed ferritin levels of around 3000 ng/mL, none of them showed marked reduction of LVEF, except patient 5 who was given a diagnosis of aplastic anemia in childhood and in whom the exact transfused RBC amount could not be calculated.

Because of blurring artifacts, we measured cardiac T2* value in 6 patients. Breath holding was difficult for patient no. 2 and we therefore failed to establish the ROI in the myocardium of this patient. Although the number of patients in this study is too small to provide a definite conclusion, we were able to note some tendencies regarding iron overload in the heart. Two patients (nos. 1 and 6) who received relatively small amounts of RBC transfusions (approximately 60 Japanese units: 12,000 mL) had normal T2* value, suggesting that at 60 units RBC (200 mL/kg) transfusion myocardial iron overload may not occur. Most patients with RBC transfusion of 60–120 units (200–400 mL/kg) maintained normal LVEF, while some of them demonstrated mild reduction in T2* value (35.71 ms and 35.59 ms); but the above 2 patients (nos. 3 and 7) with 60 units of transfusion showed the limit of the normal range T2* value reported by Anderson et al., i.e., 52 ± 16 ms [7]. These data indicate that some patients with heavy transfusion of 60–120 RBC Japanese units (12,000–24,000 mL RBC) may not be detectable myocardial damage by LVEF alone, and the T2* value of MRI could show cardiac iron deposition before the appearance of myocardial dysfunction.

We utilized GraphPad Prism 5.0 software (GraphPad Software Inc., San Diego, CA, USA) to obtain non-lineal fitting capabilities between total transfused RBC volume and serum ferritin, T2* value, or ejection fraction by MRI (Fig. 1).

(1) *No obvious cardiac siderosis*: patients with RBC transfusion of <200 mL/kg (<12,000 mL RBC) exhibiting elevated serum ferritin up to 4000 ng/mL, normal T2* value (36–68 ms), and normal LVEF (56–78% by MRI).
(2) *Cardiac siderosis*: patients with RBC transfusion of 200–400 mL/kg (12,000–24,000 mL RBC) exhibiting elevated serum ferritin up to 4000 ng/mL, progressive reduction of the T2* value, and normal LVEF (56–78% by MRI).
(3) *Cardiac dysfunction due to siderosis*: patients with RBC transfusion of >400 mL/kg (>24,000 mL) exhibiting elevated serum ferritin levels of more than 15,000 ng/mL, reduced T2* value (<20 ms), and abnormal LVEF (<56% by MRI).

4. Discussion

In the current study, we failed to demonstrate a linear correlation between the T2* value and left ventricular ejection fraction, especially in patients with transfusion of less than 120 Japanese units of RBC (<400 mL/kg). Approximately 50% of them showed some reduction of T2* value, while most of them exhibited a normal LVEF, indicating that these high transfusion level patients are at high risk for developing cardiac dysfunction, and detection of insidiously progressive dysfunction detected by MRI might be important for those patients. The situation is similar in those with serum ferritin levels between 2000 ng/mL and 4000 ng/mL: evaluation of LVEF alone by echocardiogram may fail to find out the pre-existing myocardial damage due to iron overload.

The T2* value is related to not only iron deposition but also fibrosis, and MRI reflects total images of these pathologic changes. Currently iron chelation therapy for hematologic disease patients, especially those with myelodysplastic syndromes (MDS), with transfusion-dependency is recommended [3], and definitions of iron overload for MDS patients have been proposed [8,9]. Although the starting point for iron chelation therapy is proposed, the exact evaluation of iron overload and functional estimation in each organ is probably important. Reduction of iron deposition in mouse organs by chelation therapy was demonstrated [10]. Thus, improvement of cardiac siderosis and myocardial dysfunction by chelation therapy should be determined.

Anderson et al. reported cardiac iron deposition in 109 thalassemia patients with iron chelation therapy and found significant ventricular dysfunction in patients with myocardial T2* values of less than 20 ms, and progressive decline in ejection fraction [7].

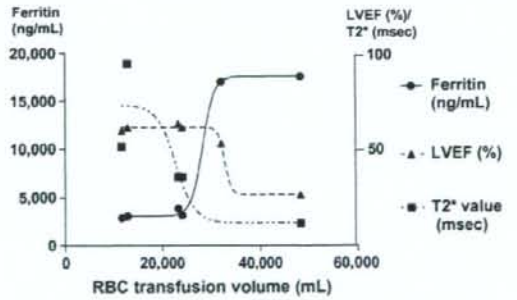

Fig. 1. Correlation between total units of red blood cell transfusion (horizontal axis) and left ventricular ejection fraction (LVEF), serum ferritin, and cardiac T2* value using GraphPad Prism 5.0 software. Rapid decline of T2* value, but stable LVEF within the normal range until 400 mL/kg of red blood cell transfusion and serum ferritin level of <5000 ng/mL are notable. The rapid decline of LVEF following rapid elevation of serum ferritin is evident.

Please cite this article in press as: Park J, et al. Evaluation of cardiac iron overload in transfusion-dependent adult marrow failure patients by magnetic resonance imaging. Leuk Res (2008), doi:10.1016/j.leukres.2008.10.018

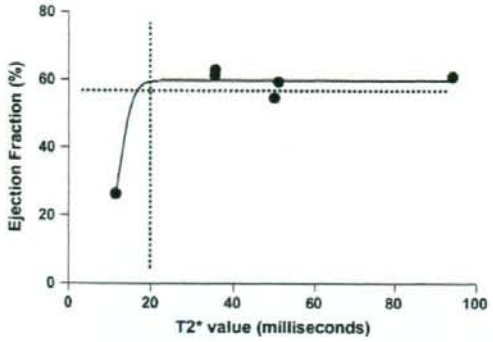

Fig. 2. Correlation between cardiac T2* value and left ventricular ejection fraction. The vertical dotted line indicates the cut-off value of T2* (20 ms) and the horizontal dotted line shows the cut-off value of LVEF (56%) for cardiac dysfunction.

In contrast, Jensen et al. failed to demonstrate significant correlation between cardiac T2* value and serum ferritin levels [5]. More recently, Di Tucci et al. reported myocardial iron overload detected by MRI in adult transfusion-dependent acquired anemias and found cardiac T2* value correlated with transfusion burden, and suggested that 290 mL/kg RBC might be a cut-off for myocardial damage [6]. Our results show that patients who received transfusions of up to 24,000 mL RBC (approximately 400 mL/kg) had a progressive decrease of the T2* value, but most of them had a normal left ventricular ejection fraction. These data clearly indicate that patients receiving 200–400 mL/kg RBC transfusion with moderate reduction of T2* value, but not less than 20 ms, in acquired anemia patients with heavy transfusion may be at high risk for progressive cardiac dysfunction (Fig. 2).

In conclusion, RBC transfusion of 200 mL/kg RBC might be the limit for monitoring normal T2* values. Patients who received 200–400 mL/kg RBC transfusion showed progressive decrease of T2* value without obvious reduction of ejection fraction, indicating that the T2* value of MRI could indicate cardiac iron deposition before apparent myocardial dysfunction. Patients who had received ≥400 mL/kg RBC transfusion eventually showed progressive cardiac failure.

Conflicts of interest

The authors declare no conflicts of interests.

Acknowledgements

Thanks are due to Prof. J. Patrick Barron, salaried employer of Tokyo Medical University, for his review of this manuscript. We also thank to Mr. H. Katsuyama and Y. Araki, Department of Radiology, Tokyo Medical University, Y. Komori, Siemens-Asahi Medical Technologies Ltd., Japan, for their technical help and Dr. J. H. Ohyashiki, Intractable Diseases Research Center, for statistical analysis. This work was supported in part by a Grant-in-Aid from Japanese Ministry of Health, Labor and Welfare.

References

[1] Takatoku M, Uchiyama T, Okamoto S, et al. Japanese National Research Group on Idiopathic Bone Marrow Failure Syndromes. Retrospective nationwide survey of Japanese patients with transfusion-dependent MDS and aplastic anemia highlights the negative impact of iron overload on morbidity/mortality. Eur J Haematol 2007;78:487–94.
[2] Konen E, Ghoti H, Goitein O, et al. No evidence for myocardial iron overload in multitransfused patients with myelodysplastic syndrome using cardiac magnetic resonance T2 technique. Am J Hematol 2007;82:1013–6.
[3] Greenberg PL. Myelodysplastic syndromes: iron overload consequences and current chelating therapies. J Natl Compr Cancer Netw 2006;4:91–6.
[4] Chacko J, Pennell DJ, Tanner MA, et al. Myocardial iron loading by magnetic resonance imaging T2* in good prognostic myelodysplastic syndrome patients on long-term blood transfusions. Br J Haematol 2007;138:587–93.
[5] Jensen PD, Jensen FT, Christensen T, et al. Evaluation of myocardial iron by magnetic resonance imaging during iron chelation therapy with deferrioxamine: indication of close relation between myocardial iron content and chelatable iron pool. Blood 2003;101:4632–9.
[6] Di Tucci AA, Matta G, Deplano S, et al. Myocardial iron overload assessment by T2* magnetic resonance imaging in adult transfusion dependent patients with acquired anemias. Haematologica 2008;93:1358–8.
[7] Anderson LJ, Holden S, Davis B, et al. Cardiovascular T2-star (T2*) magnetic resonance for the early diagnosis of myocardial iron overload. Eur Heart J 2001;22:2171–9.
[8] Gatterman N. Guidelines on iron chelation therapy in patients with myelodysplastic syndromes and transfusional iron overload. Leuk Res 2007;(Suppl. 3):S10–5.
[9] Suzuki T, Tomonaga M, Miyazaki Y, et al. Japanese epidemiological survey with consensus statement on Japanese guidelines for treatment of iron overload in bone marrow failure syndromes. Int J Hematol 2008;88:30–5.
[10] Wood JC, Otto-Duessel M, Gonzalez I, et al. Deferasirox and deferiprone remove cardiac iron in the iron-overload gerbil. Transl Res 2006;148:272–80.

Please cite this article in press as: Park J, et al. Evaluation of cardiac iron overload in transfusion-dependent adult marrow failure patients by magnetic resonance imaging. Leuk Res (2008), doi:10.1016/j.leukres.2008.10.018

Int J Hematol (2008) 88:73–81
DOI 10.1007/s12185-008-0115-2

ORIGINAL ARTICLE

A safety, pharmacokinetic and pharmacodynamic investigation of deferasirox (Exjade®, ICL670) in patients with transfusion-dependent anemias and iron-overload: a Phase I study in Japan

Keisuke Miyazawa · Kazuma Ohyashiki · Akio Urabe · Tomoko Hata · Shinji Nakao · Keiya Ozawa · Takayuki Ishikawa · Junji Kato · Yoichi Tatsumi · Hiraku Mori · Midori Kondo · Junsuke Taniguchi · Hiromi Tanii · Lisa Rojkjaer · Mitsuhiro Omine

Received: 19 March 2008 / Revised: 26 April 2008 / Accepted: 29 May 2008 / Published online: 4 July 2008

Abstract The pharmacokinetics (PK) and pharmacodynamics (PD) of the once-daily, oral ironchelating agent, deferasirox (Exjade®, ICL670), have been evaluated further in a Phase I, openlabel, multicenter, dose-escalation study in Japanese patients with myelodysplastic syndromes, aplastic anemia, and other anemias. Deferasirox was initially administered as a single dose of 5 ($n = 6$), 10 ($n = 7$), 20 ($n = 6$) or 30 ($n = 7$) mg/(kg day) and then after 7 days seven daily doses were administered. Linear PK (C_{max} and AUC) were observed at all doses after a single dose and at steady state, and dose-dependent iron excretion was observed. Pharmacokinetic/pharmacodynamic parameters were similar to those reported in a Caucasian β-thalassemia cohort. Following the single- and multiple-dose phases, 21 of 26 patients progressed to a 3-year extension phase of the study, where dose reductions and increases [5–30 mg/(kg day)] were allowed following safety and efficacy assessments. In the interim, 1-year data show that deferasirox was well tolerated, with generally infrequent and mild adverse events. Reductions in serum ferritin levels were observed and a negative iron balance achieved at doses of 20–30 mg/(kg day). These data suggest that deferasirox has a stable and predictable PK/PD profile, irrespective of underlying disease or race, and a predictable and manageable safety profile suitable for chronic administration.

Keywords Iron chelation · Deferasirox · Iron overload · Myelodysplastic syndrome

K. Miyazawa (✉) · K. Ohyashiki
First Department of Internal Medicine (Hematology/Oncology), Tokyo Medical University, 6-7-1 Nishishinjuku, Shinjuku-ku, Tokyo 160-0023, Japan
e-mail: miyazawa@tokyo-med.ac.jp

A. Urabe
NTT Kanto Medical Center, Tokyo, Japan

T. Hata
Nagasaki University, Nagasaki, Japan

S. Nakao
Kanazawa University, Ishikawa, Japan

K. Ozawa
Jichi Medical University, Tochigi, Japan

T. Ishikawa
Kyoto University, Kyoto, Japan

J. Kato
Sapporo Medical University, Sapporo, Japan

Y. Tatsumi
Kinki University, Osaka, Japan

H. Mori · M. Omine
Showa University Fujigaoka Hospital, Yokohama, Japan

M. Kondo · J. Taniguchi · H. Tanii
Novartis Pharma K.K., Tokyo, Japan

L. Rojkjaer
Novartis Pharma A.G., Basel, Switzerland

1 Introduction

Blood transfusions provide key supportive therapy for patients with chronic anemias, relieving the disease symptoms, improving quality of life, and extending survival [1–3]. However, the senescence of transfused red blood cells leads to the release of excess iron for which the body has no active mechanism of removal. Once levels of transferrin, an iron-binding protein, are saturated, free iron begins to circulate and is taken up and stored in the

parenchymal cells of the liver, heart, endocrine organs, brain, and joints [4, 5]. The accumulation of toxic iron leads to the generation of active oxygen species, resulting in DNA damage, lipid peroxidation, apoptosis and, therefore, ongoing tissue damage. If iron levels remain uncontrolled, progressive organ dysfunction will result in death, principally from cardiac and liver failure. Iron overload can be effectively managed with iron chelation therapy, which can prevent the consequences of iron toxicity and improve patients' long-term outcomes [6–9].

In Japan, the myelodysplastic syndromes (MDS) and aplastic anemia (AA) are the most common anemias requiring regular blood transfusion therapy. Despite widespread recognition of the risks associated with iron overload, and the subsequent need to manage iron levels, treatment options are, at present, limited to deferoxamine (Desferal®, DFO), an iron chelator with a high molecular weight that requires parenteral administration. In contrast to most countries around the world where DFO is administered via slow subcutaneous infusion utilizing a portable pump because of its short half-life, DFO is approved in Japan only for intravenous and intramuscular administration. In contrast to the recommended regimen of slow subcutaneous infusion 5–7 nights/week, it is therefore a common practice for DFO to be administered only once every 2 weeks in a hospital setting. As studies have demonstrated that chelation coverage is limited to periods of drug exposure, infrequent infusions will allow raised levels of non-transferrin bound iron to reoccur, exposing patients to toxic iron levels [10, 11]. A recent survey on Japanese patients with MDS, AA, and other anemias, highlighted that less than half had received iron chelation therapy, and of those who were treated, less than 9% received continuous/daily DFO therapy [12]. A high mortality rate was noted in this population, primarily from cardiac and liver failure, conditions commonly associated with iron overload [5, 13]. Daily or continuous iron chelation therapy was seen to effectively reduce iron burden and improve organ function [12].

Once-daily oral therapy with deferasirox (Exjade®, ICL670) has the potential to overcome the limitations of DFO treatment, providing convenient therapy and 24-h chelation coverage [14]. Registration studies conducted on non-Japanese adult and pediatric patients have demonstrated a similar efficacy to DFO at comparable doses, and dose-dependent efficacy in reducing body iron burden across a wide range of transfusion-dependent anemias [15–18]. Deferasirox has since been approved in more than 85 countries worldwide. Here, we present the findings of a Phase I clinical trial on Japanese patients with transfusion-dependent anemias treated with deferasirox in an initial pharmacokinetic (PK)/pharmacodynamic (PD) study, and interim analyses of data from the subsequent extension phase. The PK/PD parameters were compared with those previously reported in a cohort of iron-overloaded Caucasian patients with β-thalassemia [19].

2 Methods

2.1 Study objectives

The primary objective was to evaluate the tolerability and safety of deferasirox in Japanese patients with transfusional iron overload. Secondary objectives were to evaluate the PK and PD of deferasirox, including iron excretion. A comparison of the PK/PD data with those of a previously published Phase I trial (study 0104) conducted on non-Japanese β-thalassemia patients was also performed [19].

2.2 Patients

Eligible patients were ≥20 years of age, with transfusion-dependent MDS, AA or other anemias (pure red cell aplasia: PRCA, myelofibrosis: MF), having received a lifetime history of ≥35 U of packed red blood cells (RBCs). In Japan, 1 U of RBCs contains 200 mL of whole blood, and provides approximately 100 mg of iron. Serum ferritin values ≥1,000 μg/L as confirmed by at least two evaluations, during the 4 weeks prior to enrollment and an ECOG performance value of 0–2 were required. As a result, the patient with chronic inflammation, for example adult Still disease or hemophagocytic syndrome, did not enroll in this study. Patients receiving DFO therapy during the 4 weeks prior to the start of deferasirox treatment were excluded. Other parameters that excluded patients from the study at screening included alanine aminotransferase (ALT) levels >250 U/L, serum creatinine levels above the upper limit of normal (ULN), a urinary protein/creatinine aplastic anemia ratio >0.5 mg/mg, serological evidence of chronic hepatitis B virus infection, clinical evidence of active hepatitis C virus infection, uncontrolled gastrointestinal problems (diarrhea, constipation, or bleeding), and cataract or a previous history of clinically relevant ocular dysfunction related to iron chelation. All patients provided written informed consent.

The study by Nisbet-Brown et al. [19] (Study 0104), which was used for comparison, enrolled Caucasian patients (male and female, aged ≥16 years) with β-thalassemia and transfusional iron overload.

2.3 Study design and dosing

This Phase I, collaborative, openlabel, non-blind, dose-escalation study was conducted in nine centers in Japan. The study was conducted in three phases, a single-dose phase (1-day treatment in each dose cohort), a multiple-dose

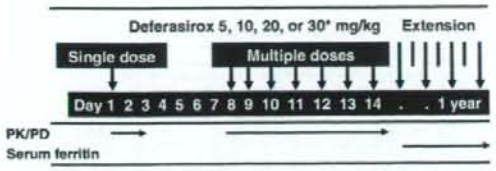

Fig. 1 Study design indicating dosing and PK/PD assessments. *Asterisk* denotes cohort commenced treatment on 20 mg/(kg day) in the extension

phase (7-day treatment in each dose cohort), and an extension phase (1-year data reported; Fig. 1). Single dosing was initiated with a cohort treated at 5 mg/kg. Efficacy and Safety Committee review subsequently approved enrollment of the next dosing cohort (10, 20, and 30 mg/kg) and progression to the multiple-dose phase where patients received daily doses of deferasirox 30 min before breakfast. Deferasirox dosing was based on previous studies in Caucasian populations [19, 20]. Patients were hospitalized during the single- and multiple-dose periods and given a standard low iron diet from day 1 to day 14. In study 0104, deferasirox was administered at 10, 20, and 40 mg/kg once daily for 12 days [19].

Following completion of the single- and multiple-dose phases of the study, treatment could continue into the extension phase for approximately 3 years at the patient's request in the ethical point of view for patient. Following Efficacy and Safety Committee review, a recommendation to adjust deferasirox dose in relation to transfusion requirement was made. As a result, patients receiving deferasirox 5, 10 or 20 mg/(kg day) continued into the extension phase at the same doses, but those who had originally received 30 mg/(kg day) began the extension phase on 20 mg/(kg day) to avoid potential over chelation. Dose adjustment was subsequently allowed to 30 mg/(kg day) in the extension phase following a trend of increasing serum ferritin levels or increased frequency of blood transfusion. Dose was decreased down to 5 mg/(kg day) in cases of increasing serum creatinine levels, adverse events (AEs) or decreases in serum ferritin level. Dose reduction or interruptions were implemented for skin rash, increase in serum creatinine, and increase in urinary protein/creatinine ratio. If serum ferritin fell to $\leq$500 μg/L on two consecutive study visits, treatment was interrupted until serum ferritin was >1,000 μg/L.

2.4 Safety assessments

Safety evaluations were based on reports of AEs and serious AEs, plus assessment of hematology, blood chemistry, urinalysis, vital signs, physical examinations, electrocardiograms, and ocular and audiometry examinations.

2.5 Pharmacokinetic/pharmacodynamic evaluation

Pharmacokinetic/pharmacodynamic assessments were made during the single- and multiple-dose phases. Pharmacokinetic calculations were based on free deferasirox and the iron-complex of deferasirox (Fe-[ICL670]$_2$) by means of a non-compartmental analysis to determine t_{max}, C_{max}, AUC_{0-24}, and $t_{1/2}$. Total iron excretion was calculated as the sum of the urinary and fecal iron excretion. Iron excretion induced by deferasirox was calculated as the difference between an average daily iron excretion during the treatment period (days 11, 12, 13, and 14) and an average daily iron excretion during the cessation period (days 5, 6, and 7) as the baseline value.

2.6 Markers of iron stores

During the extension phase, safety, serum ferritin, and blood biochemical tests [including albumin, alkaline phosphatase, total bilirubin, blood urea nitrogen (BUN), cholesterol, creatinine, γ-GTP, glucose, LDH, total protein, ALT, AST, triglycerides, uric acid, CRP, sodium, potassium, chloride, calcium, inorganic phosphorus, and magnesium] were evaluated monthly. Exploratory examination of changes from baseline in serum ferritin levels was conducted.

3 Results

3.1 Patient demographics

Twenty-six patients with MDS, AA or other anemias were enrolled in the single- and multiple-dose phases, all of whom completed the core phase of the study (Table 1). Twenty-one patients continued to the extension phase. Study 0104, which was used to compare the PK/PD results from the current study, enrolled nine male and nine female Caucasian patients with β-thalassemia with a median age of 26.4 years (range 18–39) [19], lower than the median age of 69.5 years (range 26–93) of the Japanese patients in the current study.

3.2 Dosing and exposure to deferasirox

All 26 patients completed the single- and multiple-dose phases. Of these 21 patients who wished to continue deferasirox treatment as extension phase, 14 (66.7%) remain on study treatment for 1 year and are continuing in the study. Those who withdrew did so primarily due to AEs or improvements in serum ferritin value that meant chelation therapy was no longer required (Table 2).

Adjustments to the starting dose were made due to insufficient efficacy of the initial dose as assessed by serum ferritin (increase in dose) and AEs (decrease in dose;

Table 1 Patient characteristics

	Deferasirox dose [mg/(kg day)]				
Core phase	5 ($n = 6$)	10 ($n = 7$)	20 ($n = 6$)	30 ($n = 7$)	Total ($n = 26$)
Median age, years (range)	71.5 (28–78)	68.0 (34–93)	66.0 (26–74)	75.0 (46–87)	69.5 (26–93)
Male:female	1:5	3:4	1:5	3:4	8:18
Underlying anemia, *n* (%)					
MDS	3 (50)	5 (71.4)	4 (66.7)	4 (57.1)	16 (61.5)
AA	3 (50)	1 (14.3)	1 (16.7)	1 (14.3)	6 (23.1)
Other anemias[a]	0	1 (14.3)	1 (16.7)	2 (28.6)	4 (15.4)

Extension phase	5 ($n = 5$)	10 ($n = 5$)	20 ($n = 11$)	Total ($n = 21$)
Median age, years (range)	70.0 (28–77)	68.0 (34–78)	68.0 (26–76)	68.0 (26–78)
Male:female	1:4	2:3	3:8	6:15
Underlying anemia, *n* (%)				
MDS	2 (40.0)	3 (60.0)	7 (63.6)	12 (57.1)
AA	3 (60.0)	1 (20.0)	2 (18.2)	6 (28.6)
Other anemias[b]	0	1 (20.0)	2 (18.2)	3 (14.3)
Blood intake during the extension phase, median units/month[c] (range)	4.4 (0–9.6)	4.3 (0–6.1)	3.9 (3.0–13.2)	4.4 (0–15.7)

MDS, myelodysplastic syndromes; *AA*, aplastic anemia

[a] Other anemias: pure red cell aplasia ($n = 3$), myelofibrosis ($n = 1$)

[b] Other anemias: pure red cell aplasia ($n = 2$), myelofibrosis ($n = 1$)

[c] 1 unit = 200 mL

Table 2). As a result of the criteria of dose reduction and interruption shown in Sect. 2.3, dosing was reduced and interrupted in five (23.8%) and eight (38.1%) patients, respectively, because of adverse events (AEs). Seven patients (33.3%) stopped treatment during the extension phase: four (19.0%) because of AEs; two (9.5%) because of improvements in their serum ferritin values; and one (4.8%) because of insufficient nutrition due to family circumstances. In study 0104, five, six, and seven patients were dosed with deferasirox 10, 20, and 40 mg/(kg day), respectively [19].

3.3 Safety and tolerability

Deferasirox was generally well tolerated, and reported AEs were infrequent and mild in severity. No deaths were reported during the study. In the single- and multiple-dose phase, the most common AEs with a reported relationship to deferasirox were diarrhea [7.7%; $n = 2$ each after single and multiple doses of 30 mg/(kg day)], nausea [7.7%; $n = 1$ each after multiple doses at 10 and 30 mg/(kg day)], and non-progressive increases in serum creatinine [7.7%;

Table 2 Duration of treatment, dose adjustments, and discontinuations during the extension phase

	Deferasirox dose [mg/(kg day)]			
	5 ($n = 5$)	10 ($n = 5$)	20 ($n = 11$)	Total ($n = 21$)
Median treatment duration, days (range)	361 (231–365)	365 (197–365)	365 (71–374)	365 (71–374)
Dose adjustments				
Increase, *n* (%)	3 (60.0)	3 (60.0)	1 (9.1)	7 (33.3)
Decrease due to AEs, *n* (%)	0	0	5 (45.5)	5 (23.8)
Interruption due to AEs, *n* (%)	2 (40.0)	2 (40.0)	4 (36.4)	8 (38.1)
Interruption due to symptom improvement, *n* (%)	1 (20.0)	0	2 (18.2)	3 (14.3)
Discontinuations				
Symptom improvement, *n* (%)	1 (20.0)	1 (20.0)	0	2 (9.5)
AEs, *n* (%)	1 (20.0)	1 (20.0)	2 (18.2)	4 (19.0)
Family circumstances[a], *n* (%)	1 (20.0)	0	0	1 (4.8)

AEs, adverse events

[a] Insufficient nutrition

$n = 1$ each after multiple doses at 5 and 30 mg/(kg day)]. One of the 26 patients (3.8%) had two serious AEs, pyrexia and duodenal ulcer, during the multiple-dose phase after doses of 30 mg/(kg day). A relationship with study drug could not be excluded as a cause of this event, although the patient had experienced occasional upper GI symptoms before starting the study.

During the extension phase, the most common AEs with a reported relationship to deferasirox were non-progressive increases in serum creatinine (>33% from baseline value or >ULN at two consecutive visits), increased urine β2-microglobulin, and increased blood alkaline phosphatase (Table 3). Increases in serum creatinine were seen most frequently in the 20 mg/kg dose group, 4–8 weeks after the start of treatment. In patients with increased serum creatinine, a dose reduction or interruption was required most frequently in patients in the higher (20 mg/kg) dose group whose amount of blood transfusion was low [<7 mL/(kg month)].

One of the 21 patients receiving deferasirox 20 mg/(kg day) had a transient increase in liver transaminase levels. Deferasirox treatment was interrupted for 1 week, which led to a reduction in transaminase levels. Deferasirox was restarted at 20 mg/(kg day), and no subsequent increase in transaminases was observed; treatment continued at the same dose.

There were two serious AEs with a suspected relationship to deferasirox administration, both in patients treated at 20 mg/(kg day): one of the 21 patients suffered pharyngeal ulceration and another had interstitial nephritis. Deferasirox therapy was stopped in both cases. The patient with pharyngeal ulceration had a pharyngeal tumorectomy and recovered 7 months after removal from the study, while in the case of interstitial nephritis, the patient's serum creatinine and BUN improved but she was removed from the study 10 weeks after the start of the treatment because her serum creatinine did not return to the initial value. Two other dose discontinuations were due to dementia and progressive multifocal leukoencephalopathy, and these were unrelated to study drug.

3.4 Pharmacokinetic and pharmacodynamic evaluation

3.4.1 Pharmacokinetic evaluation

After single and multiple doses (at steady state), dose-proportional C_{max} and AUC were observed (Table 4; Fig. 2). At steady-state, C_{max} and AUC were approximately 1–2-fold higher than following single-dose administration. The PK parameters (C_{max} and AUC) of deferasirox measured in these Japanese patients were

Table 3 Treatment-related adverse events occurring in ≥2 patients in the extension phase

	Initial deferasirox dose [mg/(kg day)]			
	5 ($n = 5$)	10 ($n = 5$)	20 ($n = 11$)	Total ($n = 21$)
Total adverse drug reactions, *n*	0	1 (20.0)	10 (90.9)	11 (52.4)
Increased serum creatinine[a], *n* (%)	0	0	6 (54.5)	6 (28.6)
Increased urine β2-microglobulin, *n* (%)	0	0	4 (36.4)	4 (19.0)
Increased serum alkaline phosphatase, *n* (%)	0	0	3 (27.3)	3 (14.3)

[a] Non-progressive increase >33% from baseline value or >ULN at two consecutive visits

Table 4 Pharmacokinetic parameters of deferasirox after the single- and multiple-dose phases

Dose (mg/kg)	t_{max} (h)	C_{max} (μmol/L)	AUC_{0-24} (μmol h/L)	$t_{1/2}$ (h)
Day 1 (single dose)				
5 ($n = 6$)	2.0 (0.9–3.0)	20.4 ± 6.1	190 ± 91	8.5 ± 3.4
10 ($n = 7$)	3.0 (1.0–4.0)	53.3 ± 18.7	535 ± 137	17.1 ± 4.7
20 ($n = 6$)	4.0 (1.0–10.0)	112 ± 29	1,270 ± 366	20.5 ± 4.9
30 ($n = 7$)	3.0 (2.0–4.0)	119 ± 40	1,450 ± 423	18.9 ± 9.8[a]
Day 14 (multiple dose)				
5 ($n = 6$)	1.5 (1.0–4.0)	27.4 ± 10.7	345 ± 236	17.5 ± 7.2
10 ($n = 7$)	3.0 (1.1–10.0)	67.3 ± 22.2	848 ± 442	20.5 ± 7.5
20 ($n = 6$)	3.4 (1.0–4.2)	119 ± 14	1,510 ± 193	21.4 ± 7.2
30 ($n = 7$)	3.9 (1.0–10.0)	224 ± 100	3,620 ± 2,760	19.5 ± 4.9

Mean ± SD except for t_{max} [median (min–max)]

[a] $n = 6$

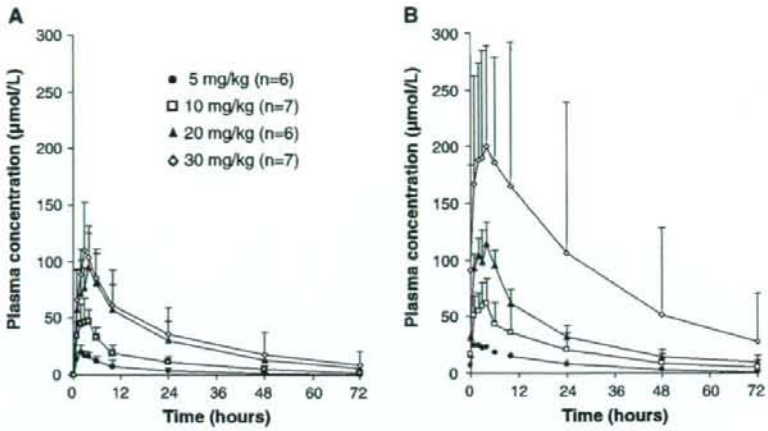

Fig. 2 Plasma concentration–time profiles of deferasirox after **a** single dosing (day 1) and **b** multiple dosing (day 14)

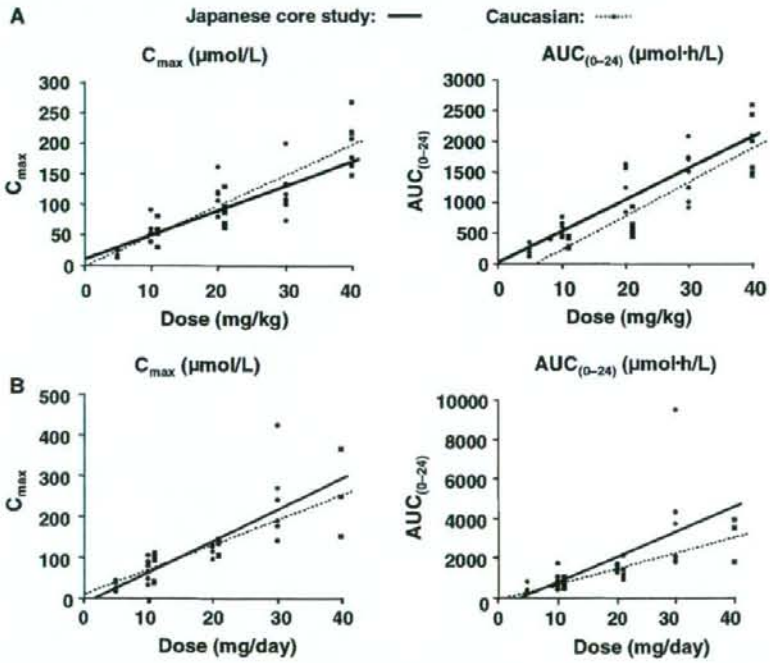

Fig. 3 pharmacokinetics–dose relationship in Japanese (data from current study) and Caucasian patients [19] (data from study 104) after **a** single dosing (day 1) and **b** multiple dosing (day 14)

similar to those measured in Caucasian patients in study 0104 (Fig. 3) [19].

3.4.2 Pharmacodynamic evaluation

One patient in the 5 mg/kg dosing group experienced fecal occult blood and was excluded from the PD data analysis. Dose-dependent iron excretion and a linear relationship between PK (AUC) and PD (iron excretion) were observed (Table 5), with iron excretion being similar to that measured in the Caucasian patients in study 0104 (range 0.12–0.45 mg iron/(kg day); Figs. 4, 5).

3.5 Changes in serum ferritin levels

Changes in levels of serum ferritin were assessed as a marker of iron stores. At the start of the extension phase, median serum ferritin levels were 4,500 μg/L (range

Table 5 Iron excretion

Dose (mg/kg)	Mean iron excretion rate ± SD [mg/(kg day)]		
	Fecal iron excretion	Urinary iron excretion	Total iron excretion
5 ($n = 6$)	0.07 ± 0.10	0.01 ± 0.00	0.07 ± 0.10
10 ($n = 7$)	0.12 ± 0.12	0.01 ± 0.00	0.13 ± 0.12
20 ($n = 6$)	0.33 ± 0.12	0.02 ± 0.00	0.34 ± 0.12
30 ($n = 7$)	0.58 ± 0.39	0.02 ± 0.01	0.61 ± 0.39

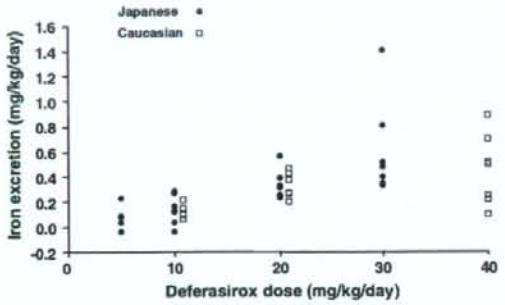

Fig. 4 Dose-related iron excretion in Japanese (data from current study) and Caucasian patients [19] (data from study 104)

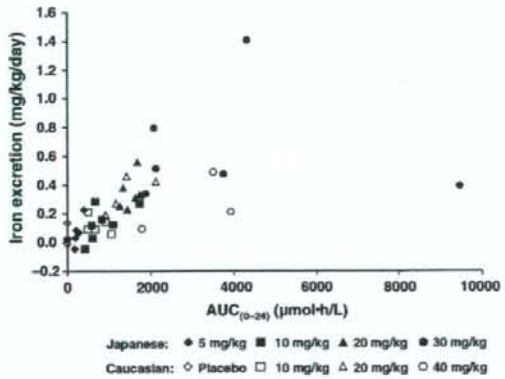

Fig. 5 Relationship between PK and PD in Japanese (data from current study) and Caucasian patients [19] (data from study 104)

1,400–17,000). After 1 year, all patients in the 20 mg/(kg day) group had a decrease in their serum ferritin levels, indicating a negative iron balance, as did four of five patients in the 10 mg/(kg day) group and two of five patients in the 5 mg/(kg day) group. However, these results include dose increases according to the dose adjustment protocol: in the 5 mg/(kg day) group, two patients were increased to 10 mg/(kg day) and one patient was increased

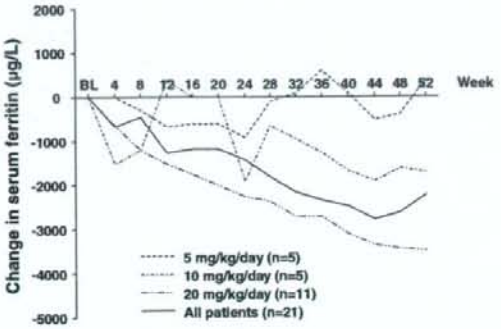

Fig. 6 Changes in serum ferritin following administration of deferasirox. Dose was increased according to the dose adjustment protocol: in the 5 mg/(kg day) group, two patients were increased to 10 mg/(kg day) and one patient was increased to 20 mg/(kg day); in the 10 mg/(kg day) group, three patients were increased to 20 mg/(kg day); and in the 20 mg/(kg day) group, one patient was increased to 30 mg/(kg day)

Table 6 The value of serum ferritin in baseline and after 1 year of deferasirox

Dose (mg/kg)	Mean value of serum ferritin ± SD (μg/L)			
	Baseline		After 1 year (52 weeks)	
5 ($n = 5$)	($n = 5$)	3,700 ± 2,203	($n = 3$)	4,267 ± 1,012
10 ($n = 5$)	($n = 5$)	7,040 ± 5,719	($n = 3$)	4,533 ± 1,747
20 ($n = 11$)	($n = 11$)	4,309 ± 1,865	($n = 8$)	1,243 ± 496
All ($n = 21$)	($n = 21$)	4,814 ± 3,307	($n = 14$)	2,596 ± 1,843

to 20 mg/(kg day); in the 10 mg/(kg day) group, three patients were increased to 20 mg/(kg day); and in the 20 mg/(kg day) group, one patient was increased to 30 mg/(kg day). The median serum ferritin level after 1 year of deferasirox treatment fell by 3,485 μg/L in the 20 mg/(kg day) group and by 1,700 μg/L in the 10 mg/(kg day) group; the median serum ferritin level rose by 400 μg/L in the 5 mg/(kg day) group (Fig. 6). The mean values of serum ferritin at each dose of deferasirox in baseline and after 1 year of deferasirox treatment is shown in Table 6.

4 Discussion

Deferasirox is a once-daily oral iron chelator that allows flexible dosing, adjustable to transfusional iron intake, and therapeutic goal (decrease or maintenance of total body iron). This study assessed the safety, PK, and PD of deferasirox in Japanese patients with chronic anemias and transfusion-dependent iron overload in order to compare with data obtained in Caucasian patients with transfusion-dependent β-thalassemia and secondary iron overload [19].

Deferasirox was generally well tolerated with a manageable safety profile after daily dosing for up to 1 year. The incidence and severity of AEs related to study treatment appeared to be dose dependent, although low patient numbers in each group limit a conclusion. The AE profile in Japanese patients was similar to that seen in previous studies of Caucasian patients with MDS, with no additional safety concerns [15]. Potential AEs in Japanese patients could, therefore, be expected to be anticipated and managed in a similar way to those in non-Japanese patients [21]. Mild increase of serum creatinine to >33% above baseline levels and interstitial nephritis has been observed in the patients treated at 20 mg/kg. After the initial increase, the creatinine levels have remained stable and transient increases in the urinary excretion of β2-microglobulin were observed in some patients. These findings may relate to pre-existing proximal renal tubular damage, which has been attributed to the toxic effects of iron deposits in the kidneys. Investigations are ongoing to explore the effects of deferasirox on the kidney. Meanwhile, serum creatinine should be monitored monthly in all patients.

Exposure to deferasirox was dose dependent with a linear PK/PD relationship, resulting in dose-dependent iron excretion. The PK/PD parameters in the Japanese patients were similar to those seen in the Nisbet-Brown et al. Caucasian β-thalassemia cohort (Study 0104), suggested that deferasirox has a stable and predictable PK/PD, regardless of underlying disease or race. Although efficacy was not evaluated in this study, assessment of serum ferritin levels as an indicator of iron stores indicates that the high iron load of this patient population was reduced after 1 year's deferasirox therapy, and a negative iron balance was achieved in the 20 mg/(kg day) dose group. In a previous study of deferasirox in non-Japanese patients with MDS, and a similar mean iron intake level to the Japanese patients in the current study, doses of 20 and 30 mg/(kg day) were also shown to maintain or reduce iron levels.

In conclusion, this study demonstrates that the PK/PD profile of deferasirox in iron-overloaded Japanese patients with transfusion-dependent anemias is consistent with that previously reported in Caucasian patients [19], with safety and tolerability profiles similar to previous deferasirox studies [21].

References

1. Olivieri N. Thalassaemia: clinical management. Baillieres Clin Haematol. 1998;11:147–62.
2. Jansen AJ, Essink-Bot ML, Beckers EA, Hop WC, Schipperus MR, Van Rhenen DJ. Quality of life measurement in patients with transfusion-dependent myelodysplastic syndromes. Br J Haematol. 2003;121:270–4.
3. Lee MT, Piomelli S, Granger S, et al. Stroke prevention trial in sickle cell anemia (STOP): extended follow-up and final results. Blood. 2006;108:847–52.
4. McLaren GD, Muir WA, Kellermeyer RW. Iron overload disorders: natural history, pathogenesis, diagnosis, and therapy. Crit Rev Clin Lab Sci. 1983;19:205–66.
5. Kushner JP, Porter JP, Olivieri NF. Secondary iron overload. Hematology Am Soc Hematol Educ Program. 2001;47–61.
6. Gabutti V, Piga A. Results of long-term iron-chelating therapy. Acta Haematol. 1996;95:26–36.
7. Olivieri NF, Nathan DG, MacMillan JH, et al. Survival in medically treated patients with homozygous β-thalassemia. N Engl J Med. 1994;331:574–8.
8. Olivieri NF, Brittenham GM. Iron-chelating therapy and the treatment of thalassemia. Blood. 1997;89:739–61.
9. Cortelezzi A, Cattaneo C, Cristiani S, et al. Non-transferrin-bound iron in myelodysplastic syndromes: a marker of ineffective erythropoiesis? Hematol J. 2000;1:153–8.
10. Porter JB, Abeysinghe RD, Marshall L, Hider RC, Singh S. Kinetics of removal and reappearance of non-transferrin-bound plasma iron with deferoxamine therapy. Blood. 1996;88:705–13.
11. Cabantchik ZI, Breuer W, Zanninelli G, Cianciulli P. LPI-labile plasma iron in iron overload. Best Pract Res Clin Haematol. 2005;18:277–87.
12. Takatoku M, Uchiyama T, Okamoto S, et al. Retrospective nationwide survey of Japanese patients with transfusion-dependent MDS and aplastic anemia highlights the negative impact of iron overload on morbidity/mortality. Eur J Haematol. 2007;78:487–94.
13. Gattermann N, Porter JB, Lopes LF, Seymour J. Iron overload in myelodysplastic syndromes. Hematol Oncol Clin North Am. 2005;19 Suppl 1:18–25.
14. Piga A, Galanello R, Forni GL, et al. Randomized phase II trial of deferasirox (Exjade, ICL670), a once-daily, orally-administered iron chelator, in comparison to deferoxamine in thalassemia patients with transfusional iron overload. Haematologica. 2006;91:873–80.
15. Porter J, Galanello R, Saglio G, et al. Relative response of patients with myelodysplastic syndromes and other transfusion-dependent anaemias to deferasirox (ICL670): a 1-yr prospective study. Eur J Haematol. 2008;80:168–76.
16. Cappellini MD, Cohen A, Piga A, et al. A phase 3 study of deferasirox (ICL670), a once-daily oral iron chelator, in patients with β-thalassemia. Blood. 2006;107:3455–62.
17. Vichinsky E, Onyekwere O, Porter J, et al. A randomized comparison of deferasirox versus deferoxamine for the treatment of transfusional iron overload in sickle cell disease. Br J Haematol. 2007;136:501–8.
18. Galanello R, Piga A, Forni GL, et al. Phase II clinical evaluation of deferasirox, a once-daily oral chelating agent, in paediatric patients with β-thalassaemia major. Haematologica. 2006;91:1343–51.

19. Nisbet-Brown E, Olivieri NF, Giardina PJ, et al. Effectiveness and safety of ICL670 in iron-loaded patients with thalassaemia: a randomised, double-blind, placebo-controlled, dose-escalation trial. Lancet. 2003;361:1597–602.
20. Piga A, Galanello R, Cappellini MD, et al. Phase II study of ICL670, an oral chelator, in adult thalassaemia patients with transfusional iron overload: efficacy, safety, pharmacokinetics (PK) and pharmacodynamics (PD) after 18 months of therapy. Blood. 2003;102: abstr 412.
21. Vichinsky E. Clinical application of deferasirox: practical patient management. Am J Hematol. 2008;83:398–402.

[Autophagy 4:5, 629-640; 1 July 2008]; ©2008 Landes Bioscience

Research Paper

Vitamin K2 induces autophagy and apoptosis simultaneously in leukemia cells

Tomohisa Yokoyama,[1,5,†] Keisuke Miyazawa,[1, †,*] Munekazu Naito,[2] Juri Toyotake,[1] Testuzo Tauchi,[1] Masahiro Itoh,[2] Akira Yuo,[3] Yuho Hayashi,[4] Maria-Magdalena Georgescu,[4] Yasuko Kondo,[5] Seiji Kondo[5] and Kazuma Ohyashiki[1]

[1]First Department of Internal Medicine; Tokyo Medical University; [2]Department of Anatomy; Tokyo Medical University; Tokyo, Japan; [3]Department of Hematology; Research Institute; International Medical Center of Japan; Tokyo, Japan; [4]Department of Neuro-Oncology and [5]Department of Neurosurgery; The University of Texas MD Anderson Cancer Center; Houston, Texas USA

[†]These authors contributed equally to this work.

Key words: vitamin K2, autophagy, apoptosis, leukemia, acute myeloid leukemia, bcl-2

Vitamin K2 (menaquinone-4: VK2) is a potent inducer for apoptosis in leukemia cells in vitro. HL-60*bcl-2* cells, which are derived from a stable transfectant clone of the human *bcl-2* gene into the HL-60 leukemia cell line, show 5-fold greater expression of the Bcl-2 protein compared with HL-60*neo* cells, a control clone transfected with vector alone. VK2 induces apoptosis in HL-60*neo* cells, whereas HL-60*bcl-2* cells are resistant to apoptosis induction by VK2 but show inhibition of cell growth along with an increase of cytoplasmic vacuoles during exposure to VK2. Electron microscopy revealed formation of autophagosomes and autolysosomes in HL-60*bcl-2* cells after exposure to VK2. An increase of acid vesicular organelles (AVOs) detected by acridine orange staining for lysosomes as well as conversion of LC3B-I into LC3B-II by immunonoblotting and an increased punctuated pattern of cytoplasmic LC3B by fluorescent immunostaining all supported induction of enhanced autophagy in response to VK2 in HL-60*bcl-2* cells. However, during shorter exposure to VK2, the formation of autophagosomes was also prominent in HL-60*neo* cells although nuclear chromatin condensations and nuclear fragments were also observed at the same time. These findings indicated the mixed morphologic features of apoptosis and autophagy. Inhibition of autophagy by either addition of 3-methyladenine, siRNA for Atg7, or Tet-off Atg5 system all resulted in attenuation of VK2-incuded cell death, indicating autophagy-mediated cell death in response to VK2. These data demonstrate that autophagy and apoptosis can be simultaneously induced by VK2. However, autophagy becomes prominent when the cells are protected from rapid apoptotic death by a high expression level of Bcl-2.

*Correspondence to: Keisuke Miyazawa; First Department of Internal Medicine; Tokyo Medical University; 6-7-1, Nishishinjuku; Shinjuku-ku, Tokyo 160-0023 Japan; Tel.: +81.3.3342.6111, ext. 5985; Fax: +81.3.5381.6651; Email: miyazawa@tokyo-med.ac.jp

Submitted: 09/13/07; Revised: 03/19/08; Accepted: 03/20/08

Previously published online as an *Autophagy* E-publication: http://www.landesbioscience.com/journals/autophagy/article/5941

Introduction

The vitamin K family contains both natural and synthetic forms, the former including phytonadione (VK1) and the menaquinone series (VK2), and the latter including menadione (VK3). Recent studies have reported that VK2 can exert cell growth-inhibitory effects in various human cancer cells including leukemia, lung cancer and hepatocellular carcinoma (HCC) cells.[1-5] We previously reported that this cytotoxic effect of VK2 appears to be selective to leukemic blasts with almost no effects on normal hematopoietic progenitor cells.[2,6] This suggests a therapeutic advantage for using VK2 in therapy for leukemia. Several recent clinical trials demonstrated that oral administration of VK2 reduced leukemic blasts in acute myeloid leukemia (AML) and improvement of cytopenias in myelodysplastic syndromes (MDS), and also decreased the development and recurrence rates of HCC, thus improving the overall survival of patients with HCC.[7-10] Although the precise mechanism of how VK2 exerts its growth-inhibitory effects in cancer cells has not been determined, VK2 has been reported to be a potent inducer of apoptosis in various tumor cells including leukemic cells in vitro.[2,3,11-15]

Apoptosis is an evolutionally conserved, orchestrated cell-death process characterized by membrane-blebbing, DNA fragmentation, and the formation of distinct apoptotic bodies that contain components of the dead cell.[16,17] This process occurs without membrane breakdown and does not elicit an inflammatory response. Apoptotic bodies are eventually removed by phagocytic cells. Central to this apoptotic process are a group of caspases, which effect the destruction of the cell in an orderly fashion.[17] Extensive evidence suggests that therapeutic effects of various anti-cancer reagents and of radiation are mediated though apoptosis of cancer cells.[18] However, another type of caspase-independent cell death designated autophagic cell death has recently been suggested in some cancer cells in response to anticancer therapy.[19-22]

Autophagy is also an evolutionally conserved membrane trafficking process that leads to degradation of cytosolic proteins and organelles by lysosomes.[23,24] Cytosol and organelles such as mitochondria and endoplasmic reticulum are engulfed into double-membraned vesicles called autophagosomes. Fusion subsequently occurs between the

autophagosomes and lysosomes to form autolysosomes in which the cargo of the autophagosome is degraded by lysosomal hydrolases. Autophagy is induced above basal levels in response to nutrient deprivation or trophic factor withdrawal, and it sustains metabolism through the targeted catabolism of long-lived proteins. Thus, autophagy acts as a self-limited survival mechanism.[23,24] A group of genes known as Atg genes, which are conserved from yeast to humans, have been found to regulate autophagy.[25] A number of studies have reported that autophagy is activated in cancer cells derived from breast, colon, prostate and brain in response to various anticancer therapies.[21,22] Since inhibition of autophagy results in suppression of cancer cell death by anti-cancer reagents, autophagy is suggested to be a potential contributor to non-apoptotic programmed cell death.[19,21] When cell death involves autophagy, it is now designated as type II programmed cell death (PCD) or autophagic cell death, in contrast to apoptosis, which is referred to as type I PCD.[19,21] The morphological and biochemical features of autophagic cell death and apoptosis are generally distinct. In autophagic cell death, unlike apoptotic cell death, caspases are not activated, and neither DNA degradation nor nuclear fragmentation is apparent. Instead, autophagic cell death is characterized by degradation of the Golgi apparatus, polyribosomes and endoplasmic reticulum before nuclear destruction, whereas these organelles are preserved in apoptosis.[19,21] However, the involvement of autophagy in programmed cell death is still controversial, probably because the molecule(s) which execute cell death in autophagy have not been identified.[20-22]

We have previously reported that overexpression of Bcl-2 in a leukemia cell line resulted in resistance against VK2-induced apoptosis but these cells still underwent differentiation via G_1 arrest.[12] In addition, downregulation of Bcl-2 was reported to cause autophagy of HL-60 cells in a caspase-independent manner.[26] It has also been reported that Bcl-2 negatively regulates Beclin 1-depemdent autophagy and Beclin 1-dependent autophagic cell death.[27] All these data suggest the involvement of Bcl-2 in some autophagic signaling and also imply some direct or indirect interaction between mitochondria and lysosomes.[28]

In the present study, we investigated whether autophagy is involved in VK2-induced leukemic cell death using subclones of HL-60 cell line with higher and lower expression levels of the Bcl-2 protein. Our data demonstrated that both autophagy and apoptosis are simultaneously induced after VK2 treatment, but autophagy become more evident and detectable when the cells are protected from apoptosis.

Results

Bcl-2 abolished VK2-induced apoptosis but had little effect on VK2-induced growth inhibition in HL-60 cells. We have reported that treating the primary cultured leukemic cells and leukemic cell lines with 1–10 μM of VK2 for 48 to 96 hr induces apoptosis in vitro, and that the expression levels of Bcl-2 determine whether the leukemic cells to undergo apoptosis or differentiation.[2,12]

Immunoblotting with anti-Bcl-2 mAb revealed that HL-60*bcl-2* cells, which are stably transfected with human *bcl-2*, expresse Bcl-2 at a five-fold higher level than HL-60*neo* control cells (Fig. 1A). There was no difference in growth rate, morphology, and antigen expressions among the parental HL-60, HL-60*neo*, and HL-60*bcl-2* cells (data not shown). Thereafter, cell growth inhibition was assessed after 96-hr exposure to VK2 (menaquinone-4) at various concentrations. As shown in Figure 1B, VK2 inhibited HL-60 cell growth in a dose-dependent manner. HL-60*bcl-2* cells were less sensitive as compared with HL-60*neo* cells; the concentrations for the 50% growth inhibition (IC_{50}) were 6 μM for HL-60*neo* and 14 μM for HL-60*bcl-2* cells, respectively.[12] As previously reported in other leukemic cell lines and primary cultured leukemic cells,[2,11,13] treatment with 10 μM of VK2 for 72 hr potently induced apoptosis of HL-60*neo* cells as assessed by morphology, depolarization of mitochondrial membrane potential, and annexin V staining (Fig. 1C–E). In contrast, apoptosis induction by VK2 treatment was significantly suppressed in HL-60*bcl-2* cells (Fig. 1D and E), although the inhibition of cell growth was still detectable, and extended exposure to VK2 induced cell death in HL-60*bcl-2* cells (Fig. 1B). We therefore investigated whether the autophagy or non-apoptotic cell death occurred in HL-60*bcl-2* cells after treatment with VK2.

Induction of autophagy in HL-60neo/*bcl-2* cells by VK2. Since cytoplasmic vesicles became evident in HL-60*bcl-2* cells after treatment with VK2 (Fig. 1C), we first performed electron microscopy to determine whether VK2 induces autophagy in HL-60*bcl-2* cells and compared the results with those obtained with HL-60*neo* cells. As shown in Figure 2A (upper right), the nuclear degeneration and multiple chromatin bodies, which are characteristic features for the cells undergoing apoptosis, were observed in HL-60*neo* cells treated with 10 μM of VK2 for 72 hr. In contrast, numerous autophagic vacuoles and empty vacuoles were observed in HL-60*bcl-2* cells under the same conditions (Fig. 2B; upper right and lower). Most of the autophagosomes contained lamellar structures with residual digested materials. These results indicated that HL-60*bcl-2* cells treated with VK2 undergo autophagy.

It was previously reported that during amino acid starvation, LC3 becomes localized to form isolated membrane following formation of autophagosome membranes.[34] Therefore detection of the punctuated pattern of cytosolic LC3 indicates the involvement of LC3 for autophagosome formation. This phenomenon has been used as method for monitoring autophagy.[35] To further confirm the involvement of LC3 in VK2-induced autophagy, we performed fluorescent immunocytostaining of HL-60neo/*bcl-2* cells with anti-LC3B Ab and subsequent counter staining with DAPI for the detection of nuclei. As shown in Figure 3A and B, untreated HL-60*neo* and HL-60*bcl-2* cells both showed diffuse distribution of green fluorescence and no fragmented nuclei, whereas treatment with VK2 increased the punctuated pattern of LC3B in HL-60*bcl-2* cells, representing autophagic vacuoles. HL-60*neo* cells with fragmented nuclei showed no punctuated pattern of LC3B. However, in a minor population of HL-60*neo* cells without fragmented nuclei, the punctuated pattern of LC3B staining was detected. Among the cells without nuclear fragments during 72 hr-treatment with 10 μM of VK2, the percentage showing the punctuated pattern of LC3B increased in HL-60*neo* cells as well as HL-60*bcl-2* cells (Fig. 3B). This indicates that autophagy can be detected not only HL-60*bcl-2*cells but also HL-60*neo* cells. Within 48 hrs of exposure to VK2, autophagy induction was rather prominent in HL-60*neo* cells as compared with HL-60*bcl-2* cells.

Simulations induction of both apoptosis and autophagy in HL-60 cells after treatment with VK2. The data shown above suggested that both autophagy and apoptosis appear to be induced in response to VK2 in HL-60*neo* cells. For semi-quantitative assessment of the induction of autophagy, we examined the development of acid

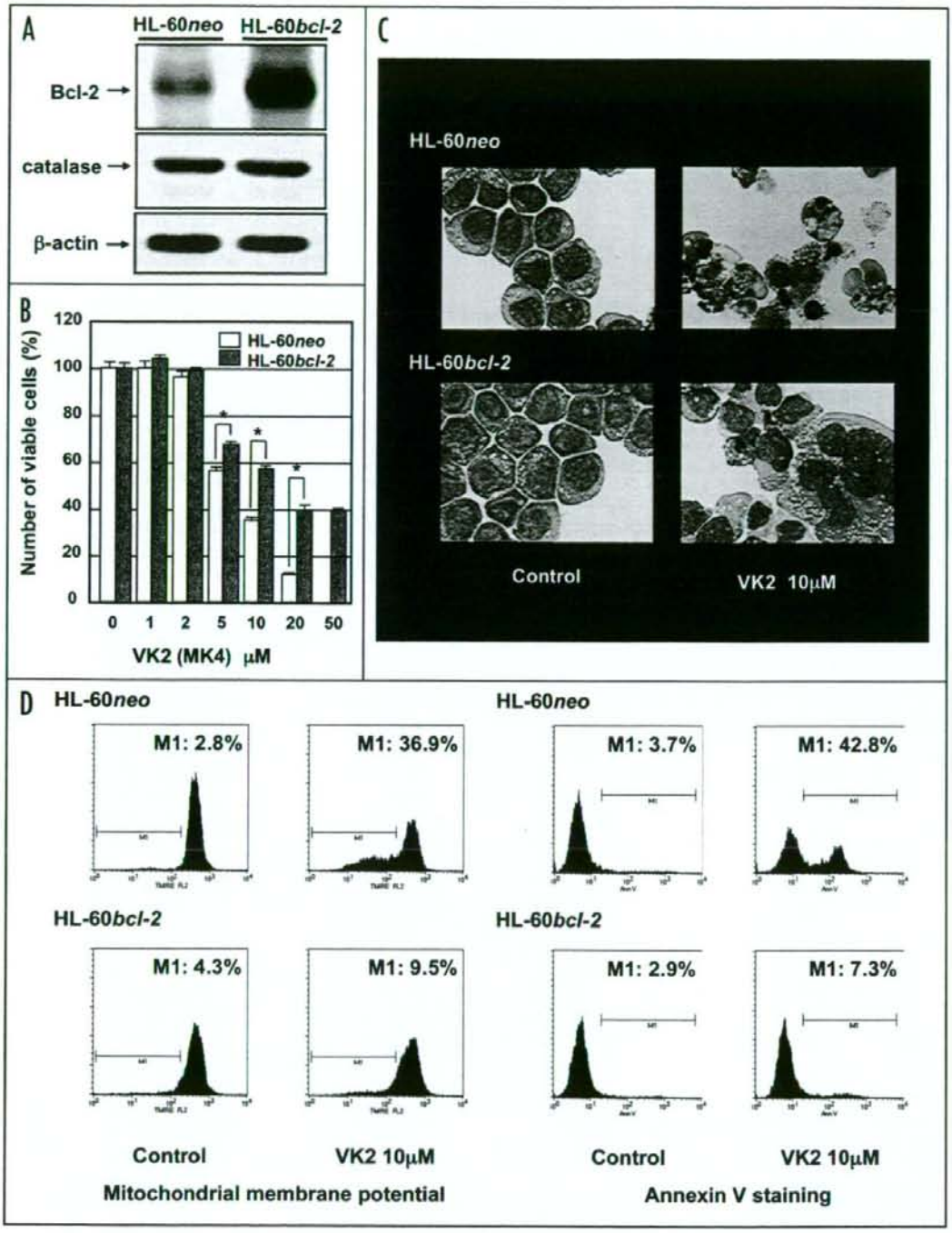

Figure 1. Inhibition of cell growth and induction of apoptosis after treatment with VK2 in HL-60 cells. (A) Expression of Bcl-2 and catalase in HL-60*neo* and HL-60*bcl-2* cells: Cellular proteins were lysed and separated by 15% SDS-PAGE for Bcl-2 and 11.25% SDS-PAGE for catalase and β-actin, and immunoblotted with anti-human Bcl-2 mAb, anti-catalase rabbit mAb, or anti-β-actin Ab, respectively. (B) Cell growth inhibition in response to VK2 in HL-60*neo*/HL-60*bcl-2* cells: Cells were cultured in the presence of various concentrations of VK2 (0.1–50 μM) for 72 hr. The number of cells was assessed with the WST cell counting kit as described in Materials and Methods. Cell growth is expressed as a ratio to the untreated control cells. *$p < 0.001$. After 72 hr exposure to 10 μM of VK2, HL-60*neo* and HL-60*bcl-2* cells were processed for (C) May-Grünwald-Giemsa staining for assessment of morphologic changes (original magnification ×1,000), and flow cytometry for (D) mitochondrial membrane potential using TMRE, and (E) Annexin V staining as described in Materials and Methods.